Multiple C−H Bond Activation: Reactions of Titanium−Phosphinimide Complexes with Trimethylaluminum

James E. Kickham, Frédéric Guérin, Jeffrey C. Stewart, Edyta Urbanska, and Douglas W. Stephan*

School of Physical Sciences, Chemistry and Biochemistry, University of Windsor, Windsor, Ontario, Canada N9B 3P4

Received December 7, 2000

Multiple C−H bond activation occurs upon reaction of phosphinimide complexes of the form Cp′(R_3PN)$TiMe_2$ (Cp′ = Cp, indenyl; R = *i*-Pr, Cy, Ph) with excess $AlMe_3$, affording the carbide complexes Cp′Ti(μ^2-Me)(μ^2-NPR_3)(μ^4-C)($AlMe_2$)$_3$ or in some cases [CpTi(μ^2-Me)(μ^2-NPR_3)(μ^5-C)($AlMe_2$)$_3$·($AlMe_3$)]. These species contain four- and five-coordinate carbide centers. VT-NMR studies established that such species exist in equilibrium. The four-coordinate carbide complexes retain Lewis acidity at a planar three-coordinate Al center, as evidenced by the reaction with diethyl ether, THF, or PMe_3. This affords species of the form [CpTi(μ^2-Me)(μ^2-NPR_3)(μ^4-C)($AlMe_2$)$_2$($AlMe_2$(L))] (L = Et_2O, THF, PMe_3). The Lewis acidity is also evidenced in the reaction of the carbide complexes with Cp$Ti(NPR_3)Me_2$. In this case, labeling studies affirm methyl group exchange processes. The analogous reactions of Cp(R_3PN)Ti(CH_2SiMe_3)$_2$ or Cp*(R_3PN)$TiMe_2$ with $AlMe_3$ afforded CpTi(μ^2-Me)(μ^2-NPR_3)(μ^3-$CSiMe_3$)($AlMe_2$)$_2$ and Cp*Ti(μ^2-Me)(μ^2-NPR_3)(μ^3-CH)($AlMe_2$)$_2$, respectively. These observations confirm that steric congestion can impinge on the C−H activation process. The nature of the above products of C−H bond activation was confirmed employing NMR, isotopic labeling, and crystallographic methods. The implications of these results with respect to C−H bond activation and polymerization catalysis are considered.

Introduction

The discovery of catalytic olefin polymerization by Ziegler and Natta some fifty years ago was the inception of what is now the huge polyolefin business. While the production of plastics is a major driving force in the world economy, the competition for quality and diversity of products continues to spur research. Over the last twenty years, well-defined "single-site catalysts" have been the subject of intense investigations.[1−6] These systems typically involve discrete early metal complexes that undergo reaction with an activator to generate the actual polymerization catalyst. Although relatively recent efforts have uncovered a variety of fluorinated-arylboron, aluminum, and metal-aryloxide based activators,[7−14] the most common activators used in commercial practice are variations of Al-based systems derived from methylalumanoxine (MAO). In our own efforts to uncover new catalyst precursors, we have recently described a variety of Ti−phosphinimide complexes that demonstrate unique and varied reactivity with different activators. For example, the complex (*t*-$Bu_3PN)_2TiMe_2$ affords a remarkably active catalyst[15] for the polymerization of ethylene upon activation with boron-based reagents. On the other hand, use of an excess of the borane $B(C_6F_5)_3$ poisons catalytic activity by formation of the bis-zwitterion (*t*-$Bu_3PN)_2$Ti(μ-MeB(C_6F_5)$_3$)$_2$.[16] Interestingly, activation of phosphinimide complexes by Al-based activators generally leads to low-activity catalysts.[15] The cause of this deviant reactivity was proposed to arise from the ability of Al reagents to react with titanium−alkyls prompting C−H bond activation. This proposition was based on the observation of C−H bond activation in the well-known Tebbe reagent, $Cp_2Ti(\mu$-$CH_2)(\mu$-Cl)$AlMe_2$,[17,18] and in the Zr and Hf clusters [(Cp*M)$_3Al_6Me_8(\mu^3$-$CH_2)_2(\mu^4$-$CH)_4(\mu^3$-CH)] described by Roesky et al.[19,20] In an effort to probe the

(1) Hlatky, G. G. *Coord. Chem. Rev.* **2000**, *199*, 235−329.
(2) Jordan, R. F. *J. Chem. Educ.* **1988**, *65*, 285−289.
(3) Yasuda, H.; Ihara, E. *Bull. Chem. Soc. Jpn.* **1997**, *70*, 1745−1767.
(4) Britovsek, G. J. P.; Gibson, V. C.; Wass, D. F. *Angew. Chem., Int. Ed.* **1999**, *38*, 428−447.
(5) Hlatky, G. G. *Coord. Chem. Rev.* **1999**, *181*, 243−296.
(6) Kaminsky, W. *J. Chem. Soc. (D)* **1998**, *009*, 1413−1418.
(7) Sun, Y.; Piers, W. E.; Rettig, S. J. *Organometallics* **1996**, *15*, 4110−4112.
(8) Chen, Y.-X.; Stern, C. L.; Marks, T. J. *J. Am. Chem. Soc.* **1997**, *119*, 2582−2583.
(9) Chen, Y.-X.; Metz, M. V.; Li, L.; Stern, C. L.; Marks, T. J. *J. Am. Chem. Soc.* **1998**, *120*, 6287−6305.
(10) Sun, Y.; Metz, M. V.; Stern, C. L.; Marks, T. J. *Organometallics* **2000**, *19*, 1625−1627.
(11) Marks, T. J. *Chem. Rev.* **2000**, *100*, 1391−1434.
(12) Chase, P. A.; Piers, W. E.; Parvez, M. *Organometallics* **2000**, *19*, 2040−2042.
(13) Williams, V. C.; Piers, W. E.; Clegg, W.; Elsegood, M. R. J.; Collins, S.; Marder, T. B. *J. Am. Chem. Soc.* **1999**, *121*, 3244−3245.
(14) Kohler, K.; Piers, W. E.; Jarvis, A. P.; Xin, S.; Feng, Y.; Bravakis, A. M.; Collins, S.; Clegg, W.; Yap, G. P. A.; Marder, T. B. *Organometallics* **1998**, *17*, 3557−3566.
(15) Stephan, D. W.; Guerin, F.; Spence, R. E. v.; Koch, L.; Gao, X.; Brown, S. J.; Swabey, J. W.; Wang, Q.; Xu, W.; Zoricak, P.; Harrison, D. G. *Organometallics* **1999**, *17*, 2046−2048.
(16) Guerin, F.; Stephan, D. W. *Angew. Chem., Int. Ed.* **2000**, *39*, 1298−1301.
(17) Tebbe, F. N.; Parshall, G. W.; Reddy, G. S. *J. Am. Chem. Soc.* **1978**, *100*, 3611−3613.

10.1021/om001047w CCC: $20.00
Publication on Web 02/20/2001

interactions of Ti−phosphinimide precatalysts and Al activators, the present article describes an investigation of the reactions of dialkyl−titanium−phosphinimide complexes with $AlMe_3$. This work demonstrates a general process of multiple C−H bond activation affording unprecedented carbide and methine Ti−Al aggregates. The implications of these results for both olefin polymerization catalysis and C−H bond activation chemistry are considered. A preliminary report of a portion of this work has been previously communicated.[21]

Experimental Section

General Data. All preparations were done under an atmosphere of dry, O_2-free N_2 employing both Schlenk line techniques and Innovative Technology or Vacuum Atmospheres inert atmosphere gloveboxes. Solvents were purified employing Grubbs type column systems manufactured by Innovative Technology. All organic reagents were purified by conventional methods. ^1H and $^{13}C\{^1H\}$ NMR spectra were recorded on Bruker Avance-300 and 500 NMR spectrometers operating at 300.13 and 500.13 MHz, respectively. Solvents were used as references, and chemical shifts are reported relative to $SiMe_4$. $^{31}P\{^1H\}$ and $^{27}Al\{^1H\}$ NMR spectra were recorded on a Bruker Avance-300 spectrometer using $AlCl_3$ in H_2O and 85% H_3PO_4 as the respective references. All NMR spectra were recorded at 25 °C unless otherwise indicated. Where applicable, variable- and low-temperature ^1H and $^{31}P\{^1H\}$ NMR studies were used to determine equilibrium constants using d_8-toluene as the solvent. The corresponding thermodynamic parameters were determined using the appropriate mathematical relationships. Guelph Chemical Laboratories Inc. of Guelph, Ontario, performed combustion analyses. Preparation of complexes of the form Cp′(R_3PN)$TiMe_2$ (Cp′ = Cp, R = Cy **1**; Cp′ = Ind, R = *i*-Pr **2**; Cp′ = Cp, R = *i*-Pr **3**; R = Ph **4**; Cp′ = Cp*, R = *i*-Pr **6**) was performed as previously described in the literature or by analogy.[15,22,23] The compound Cp(*i*-Pr_3PN)Ti(^{13}Me)$_2$ (**^{13}3**) was prepared in a similar manner employing ^{13}MeMgBr.

Synthesis of Cp(*i*-Pr_3PN)Ti(CH_2SiMe_3)$_2$, 5. To a diethyl ether solution (10 mL) of complex Cp(*i*-Pr_3PN)$TiCl_2$ (0.250 g; 0.698 mmol) was added a diethyl ether solution of Me_3SiCH_2-Li (0.70 mL; 2.0 M; 1.40 mmol) at room temperature, and the solution was stirred for 12 h. The solvent was removed in vacuo and the solid extracted with hexane (3 × 10 mL). Orange crystalline **6** was obtained by slow evaporation of the solvent. The solid was isolated by filtration and dried under vacuum (0.275 g; 0.596 mmol; 85%). ^1H NMR (C_6D_6, δ ppm): 6.25 (s, 5H, Cp-*H*); 1.72 (d of sept., $|^3J_{HH}| = 7.2$ Hz, $|^2J_{PH}| = 11.3$ Hz, 3H, PC*H*Me_2); 1.10 (d, $|^2J_{HH}| = 10.7$ Hz, 2H, C*H*$_2$-$SiMe_3$); 1.05 (d, $|^2J_{HH}| = 10.7$ Hz, 2H, C*H*$_2$-$SiMe_3$); 0.93 (dd, $|^3J_{HH}| = 7.2$ Hz, $|^3J_{PH}| = 14.7$ Hz, 18H, PCH*Me*$_2$); 0.26 (s, 18H, CH_2Si*Me*$_3$). $^{31}P\{^1H\}$ NMR (C_6D_6, δ ppm): 22.7. $^{13}C\{^1H\}$ NMR (C_6D_6, δ ppm): 110.1 (s, *Cp*); 56.5 (s, *C*H_2-$SiMe_3$); 26.4 (d, $|^1J_{PC}| = 57.5$ Hz, P*C*HMe_2); 17.2 (s, PCH(*C*H_3)$_2$); 3.5 (s, Si*Me*$_3$). Anal. Calcd for $C_{22}H_{48}NPSi_2Ti$: C, 57.24; H, 10.48; N, 3.03. Found: C, 57.04; H, 10.30; N, 3.06.

Synthesis of CpTi(μ^2-Me)(μ^2-NPCy$_3$)(μ^4-C)(AlMe2)$_3$, 7, (Indenyl)Ti(μ^2-Me)(μ^2-NP*i*-Pr_3)(μ^4-C)($AlMe_2$)$_3$, 8, CpTi(μ^2-Me)(μ^2-NP*i*-Pr_3)(μ^4-C)($AlMe_2$)$_3$(μ^2-MeAlMe_2), 9, CpTi(μ^2-Me)(μ^2-NPPh$_3$)(μ^5-C)($AlMe_2$)$_3$(μ^2-MeAlMe_2), 11, CpTi(μ^2-Me)(μ^2-NP*i*-Pr_3)(μ^3-CSiMe_3)($AlMe_2$)$_2$, 15, Cp*Ti(μ^2-Me)(μ^2-NPi-Pr_3)(μ^3-CH)($AlMe_2$)$_2$, 16. These compounds were obtained in similar manners with the appropriate precursors, and thus only one representative preparation is described. To a stirred hexane solution (10 mL) of complex **3** (0.166 g; 0.504 mmol) was added a solution of $AlMe_3$ in hexane (1.3 mL; 2.0 M; 2.60 mmol). A pale orange-beige solid precipitated from an orange solution over 24 h at room temperature. The solution was decanted from the solid, which was washed with 5 mL of hexane and dried in vacuo, yielding **9**. **7**: Precursor: **1**. Yield: 72%. ^1H NMR (C_6D_6, δ ppm): 6.22 (s, 5H, Cp-*H*); 2.01−1.01 (br m, 33H, Cy-*H*), 0.14 (br s, 3H, C*H*$_3$), −0.07 (br s, 9H, AlC*H*$_3$), −0.14 (s, 6H, AlC*H*$_3$), −0.26 (s, 3H, TiC*H*$_3$). $^{31}P\{^1H\}$ NMR (C_6D_6, δ ppm): 43.4. $^{13}C\{^1H\}$ NMR partial (C_6D_6, δ ppm): 109.8 (s, *Cp*); 37.4 (d, $|^2J_{PC}| = 12$ Hz, Cy); 27.2 (d, $|^2J_{PC}| = 36$ Hz, *Cy*), 26.7, 25.9 (s, *Cy*), −5.2 (s, Ti*Me*). **8**: Precursor: **2**. Yield: 72%. ^1H NMR (C_6D_6, δ ppm): 7.47 (d, $|^3J_{HH}| = 8.3$ Hz, 1H, *Ind*); 7.15 (m, 2H, *Ind*); 7.00 (d, $|^3J_{HH}| = 8.2$ Hz, 1H, *Ind*); 6.84 (t, $|^3J_{HH}| = 8.0$ Hz, 1H, *Ind*); 6.76 (t, $|^3J_{HH}| = 7.7$ Hz, 1H, *Ind*); 6.06 (m, 1H, *Ind*); 1.68 (d of sept., $|^3J_{HH}| = 7.1$ Hz, $|^2J_{PH}| = 13.7$ Hz, 3H, C*H*Me_2); 0.78 (dd, $|^3J_{PH}| = 14.6$ Hz, $|^3J_{HH}| = 7.3$ Hz, 9H, CH*Me*$_2$); 0.61 (dd, $|^3J_{PH}| = 15.0$ Hz, $|^3J_{HH}| = 7.3$ Hz, 9H, CH*Me*$_2$); −0.06 (s, 6H, Al*Me*$_2$); −0.14 (s, 6H, Al*Me*$_2$); −0.17 (s, 6H, Al*Me*$_2$); −0.56 (s, 3H, Ti*Me*). $^{31}P\{^1H\}$ NMR (C_6D_6, δ ppm): 51.9. $^{13}C\{^1H\}$ NMR (C_6D_6, δ ppm): 310.8 (s, Ti(*C*)Al_3); 125.3, 123.6, 123.2, 116.3, 102.8, 98.6 (s, *Ind*) 27.3 (d, $|^1J_{PC}| = 56.6$ Hz, *C*HMe_2); 16.9 (d, $|^2J_{PC}| = 44.5$ Hz, CH*Me*$_2$), 12.9 (s, Ti-*Me*); unobserved ($AlMe_x$). **9**: Precursor: **3**. Yield: 0.188 g, 67%. Compound **^{13}9** was similarly prepared from complex **^{13}3**. ^1H NMR (C_6D_6, δ ppm): 6.11 (br s, 5H, Cp-*H*); 1.78 (sept., $|^3J_{HH}| = 7.1$ Hz, 3H, PC*H*$(Me)_2$); 0.73 (dd, $|^3J_{PH}| = 14.3$ Hz, $|^3J_{HH}| = 7.1$ Hz, 9H, PCH*Me*$_2$); 0.66 (dd, $|^3J_{PH}| = 14.8$ Hz, $|^3J_{HH}| = 7.1$ Hz, 9H, PCH*Me*$_2$); 0.09 (br s, 3H, Al*Me*); −0.06 (br s, 9H, Al*Me*); −0.26 (br s, 15H, Al*Me*); −0.45 (br s, 1H, Al*Me*). $^{31}P\{^1H\}$ NMR (C_6D_6, δ ppm): 50.9 (br s). $^{13}C\{^1H\}$ NMR (C_6D_6, δ ppm): 298.2 (s, Ti(*C*)Al_3); 109.8 (s, *Cp*); 26.8 (d, $|^1J_{PC}| = 58.8$ Hz, P*C*HMe_2); 16.5 (d, $|^2J_{PC}| = 44.1$ Hz, PCH*Me*$_2$); 9.9 (s, Ti-*Me*); −0.1, −4.8, −6.1 (br s, Al-*Me*). **11**: Precursor: **4**. Yield: 64%. ^1H NMR (C_6D_6, δ ppm): 7.43 (m, 6H, C_6H_5); 7.01 (m, 9H, C_6H_5); 5.83 (s, 5H, Cp-*H*); 0.50 (br s, 3H, Ti−CH_3); −0.03 (br s, 12H, Al*Me*$_2$); −0.21 (s, 6H, Al*Me*$_2$); −0.39 (m, 9H, Al*Me*$_2$). $^{31}P\{^1H\}$ NMR (C_6D_6, δ ppm): 25.2. $^{13}C\{^1H\}$ NMR (C_6D_6, δ ppm): 134.2, 134.2, 132.1, 129.3, 127.3 (P*C*$_6H_5$); 113.2 (s, *Cp*); unobserved (Ti-*Me* and Al-*Me*). Anal. Calcd for $C_{34}H_{50}$-Al_4NPTi: C, 61.91; H, 7.64; N, 2.12. Found: C, 61.65; H, 7.37; N, 2.01. **15**: Precursor: **5**. Yield: 78%. ^1H NMR (C_6D_6, δ ppm): 6.11 (s, 5H, Cp-*H*); 1.82 (d of sept., $|^3J_{HH}| = 7.1$ Hz, $|^2J_{PH}| = 12.9$ Hz, 3H, PC*H*Me_2); 0.76 (dd, $|^3J_{PH}| = 15.0$ Hz, $|^3J_{HH}| = 7.3$ Hz, 9H, PCH(CH_3)$_2$); 0.73 (dd, $|^3J_{PH}| = 15.0$ Hz, $|^3J_{HH}| = 7.3$ Hz, 9H, PCH(CH_3)$_2$); 0.44 (s, 9H, Si*Me*$_3$); 0.06 (s, 3H, Ti*Me*); 0.05 (s, 3H, Al*Me*); −0.05 (s, 3H, Al*Me*); −0.22 (s, 3H, Al*Me*); −0.36 (s, 3H, Al*Me*). $^{31}P\{^1H\}$ NMR (C_6D_6, δ ppm): 50.2 (s, N=*P*(*i*Pr)$_3$). $^{13}C\{^1H\}$ NMR (C_6D_6, δ ppm): 110.2 (s, *Cp*); 65.9 (s, *C*H_2-$SiMe_3$); 27.2 (d, $|^1J_{PC}| = 56.2$ Hz, P*C*HMe_2); 17.2 (d, $|^2J_{PC}| = 40.1$ Hz, PCH*Me*$_3$; 5.3 (s, Si*Me*$_3$). $^{27}Al\{^1H\}$ NMR (C_6D_6, δ ppm): 65 (br). Anal. Calcd for $C_{23}H_{50}Al_2NPSiTi$: C, 55.08; H, 10.05; N, 2.79. Found: C, 54.87; H, 9.98; N, 2.66. **16**: Precursor: **6**. Yield: 80%. ^1H NMR (C_6D_6, δ ppm): 7.82 (s, 1H, Ti-C*H*-Al_2); 1.98 (m, 3H, C*H*Me_2); 1.91 (s, 15H, Cp-*Me*); 0.94 (dd, $|^3J_{HH}| = 7.3$ Hz, $|^3J_{PH}| = 14.5$ Hz, 9H, CH*Me*$_2$); 0.85 (dd, $|^3J_{HH}| = 7.4$ Hz, $|^3J_{PH}| = 14.9$ Hz, 9H, CH*Me*$_2$); −0.01 (s, 3H, Ti-*Me*); −0.16 (s, 6H, AlMe); −0.30 (s, 3H, AlMe); −0.50 (s, 3H, AlMe). $^{31}P\{^1H\}$ NMR (C_6D_6, δ ppm): 48.7. $^{13}C\{^1H\}$ NMR (C_6D_6, δ ppm): 241.8 (s, Ti-*C*H-Al_2); 119.2 (s, C_5Me_5); 28.2 (d, $|^1J_{PC}| = 56.5$ Hz, *C*HMe_2); 17.4 (d, $|^2J_{PC}| = 60.6$ Hz, CH*Me*$_2$); 12.95 (Cp-*Me*).

Synthesis of CpTi(μ^2-Me)(μ^2-NP*i*-Pr_3)(μ^4-C)($AlMe_2$)$_3$, 10 Recrystallization of **9** (or **^{13}9**) from benzene affords dark red crystalline **10** (or **^{13}10**). ^1H NMR (C_6D_6, δ ppm): 6.19 (br s, 5H, Cp-*H*); 1.84 (sept., $|^3J_{HH}| = 7.1$ Hz, 3H, PC*H*Me_2); 0.78

(18) Tebbe, F. N.; Harlow, R. L. *J. Am. Chem. Soc.* **1980**, *102*, 6151.
(19) Herzog, A.; Roesky, H. W.; Zak, Z.; Noltemeyer, M. *Angew. Chem., Int. Ed. Engl.* **1994**, *33*, 967−968.
(20) Herzog, A.; Roesky, H. W.; Jager, F.; Steiner, A.; Noltemeyer, M. *Organometallics* **1996**, *15*, 909−917.
(21) Kickham, J. E.; Guerin, F.; Stewart, J. C.; Stephan, D. W. *Angew. Chem., Int. Ed.* **2000**, *39*, 3263.
(22) Stephan, D. W.; Stewart, J. C.; Guerin, F.; Spence, R. E. v.; Xu, W.; Harrison, D. G. *Organometallics* **1999**, *18*, 1116−1118.
(23) Guérin, F.; Stewart, J. C.; Beddie, C.; Stephan, D. W. *Organometallics* **2000**, *19*, 2994.

Table 1. Crystallographic Parameters

	8	**9**	**11**	**12**	**14**	**16**
formula	$C_{31}H_{59}Al_3NPTi$	$C_{26}H_{49}Al_3NPTi$	$C_{22}H_{47}Al_3NPTi$	$C_{40}H_{53}Al_4NPTi$	$C_{25}H_{56}Al_3NP_2Ti$	$C_{25}H_{52}Al_2NPTi$
fw	605.60	535.47	485.42	734.62	561.49	499.51
a (Å)	9.61380(10)	17.499(4)	33.064(5)	18.825	18.0106(4)	9.891(2)
b (Å)	11.9618(5)	18.226(4)	36.522(7)	18.7742(3)	12.16100(10)	14.503(2)
c (Å)	15.7750(6)	21.163(6)	9.8244(19)	23.9904(4)	16.2166(3)	20.599(3)
α (deg)	92.831(2)					
β (deg)	93.736(2)	108.69(2)			107.7280(10)	94.177(8)
γ (deg)	92.541(2)					
cryst syst	triclinic	monoclinic	orthorhombic	orthorhombic	monoclinic	monoclinic
space group	$P\bar{1}$	*C*2/*c*	*Fdd*2	*Pbca*	$P2_1/c$	$P2_1/n$
vol (Å^3)	1805.98(10)	6393.7(29)	11863(4)	8479.0(2)	3383.20(10)	2946.9(7)
D_{calcd} (g cm^{-1})	1.114	1.114	1.087	1.151	1.102	1.126
Z	2	8	16	8	4	4
abs coeff, μ, mm^{-1}	0.373	0.414	0.440	0.349	0.439	0.416
data collected	8874	15 784	15 378	39 898	14 508	14 906
data $F_o^2 > 3\sigma(F_o^2)$	5860	5577	5199	7448	5180	5146
no. of variables	346	301	265	436	301	280
R (%)	8.17	6.15	4.49	5.17	7.27	3.54
R_w (%)	16.37	17.09	11.03	12.91	13.25	10.24
goodness of fit	0.941	0.999	1.104	1.034	0.988	1.010

[a] All data collected at 24 °C with Mo Kα radiation (λ = 0.71069 Å), $R = \sum||F_o| - |F_c||/\sum|F_o|$, $R_w = [\sum[w(F_o^2 - F_c^2)^2]/\sum[wF_o^2)^2]]^{0.5}$.

(dd, $|^3J_{PH}|$ = 14.8 Hz, $|^3J_{HH}|$ = 7.1 Hz, 9H, PCH*Me*$_2$); 0.72 (dd, $|^3J_{PH}|$ = 14.0 Hz, $|^3J_{HH}|$ = 7.1 Hz, 9H, PCH(C*H*$_3$)$_2$); 0.12 (br s, 3H, AlMe); −0.10 (br s, 9H, AlMe); −0.24 (br s, 9H, AlMe). ^{31}P{^{1}H} NMR (C_6D_6, δ ppm): 49.8. ^{27}Al{^{1}H} NMR (C_6D_6, δ ppm): 149 (br); 114 (br); 38 (br). ^{13}C{^{1}H} NMR (C_6D_6, δ ppm): 304.7 (s, Ti(*C*)Al$_3$); 109.9 (s, *Cp*); 27.0 (d, $|^1J_{PC}|$ = 56.6 Hz, P*C*HMe$_2$); 16.8 (d, $|^2J_{PC}|$ = 42.4 Hz, PCH(*C*H$_3$)$_2$); 10.2 (s, Ti-*C*H$_3$); −0.6, −4.5 (Al*C*H$_3$). Anal. Calcd for $C_{22}H_{47}Al_3NPTi$: C, 54.43; H, 9.76; N, 2.89. Found: C, 54.20; H, 9.39; N, 2.75.

Synthesis of [CpTi(*μ*^{2}-Me)(*μ*^{2}-NP*i*-Pr$_3$)(*μ*^{4}-C)(AlMe$_2$)$_2$-(AlMe$_2$(L))] (L = Et$_2$O 12, THF 13, PMe$_3$ 14). These compounds were obtained in similar manners with the appropriate precursors, and thus only one representative preparation is described. Complex **[13]13** was synthesized by addition of several equivalents of diethyl ether to an NMR tube containing a benzene solution of **[13]9**. **[13]12** Yield: >95% by ^{1}H NMR. ^{1}H NMR (C_6D_6, δ ppm): 6.30 (s, 5H, Cp-*H*); 3.48 (quartet, m OC*H*$_2$Me); 1.95 (sept., $|^3J_{HH}|$ = 6.8 Hz, 3H, PC*H*Me$_2$); 0.84 (t, m OCH$_2$C*H*$_3$); 0.83 (m, 18H, PCH(CH$_3$)$_2$); 0.18 (s, 3H, Al*Me*); −0.05 (s, 3H, Al*Me*); −0.08 (s, 6H, Al*Me*); −0.19 (s, 9H, Al*Me*); −0.38 (s, 3H, Al*Me*). ^{31}P{^{1}H} NMR (C_6D_6, δ ppm): 48.9. ^{27}Al{^{1}H} NMR (C_6D_6, δ ppm): 62.0 (br). ^{13}C{^{1}H} NMR (C_6D_6, δ ppm): 312.8 (s, Ti(*C*)Al$_3$); 109.9 (*Cp*); 64.9 (O*C*H$_2$Me); 27.2 (d, $|^1J_{PC}|$ = 58.8 Hz, P*C*HMe$_2$); 17.2 (d, $|^2J_{PC}|$ = 44.1 Hz, PCH(*C*H$_3$)$_2$); 13.3 (s, OCH$_2$*C*H$_3$); 10.6 (s, Ti-*C*H$_3$); −1.1, −2.4, −3.7, −4.9, −7.8 (s, AlMe). **[13]13** Yield: >95% by ^{1}H NMR. ^{1}H NMR (C_6D_6, δ ppm): 6.31 (s, 5H, Cp-*H*); 3.51 (br m, m O(C*H*$_2$CH$_2$)$_2$); 1.88 (sept., $|^3J_{HH}|$ = 7.7 Hz, 3H, PC*H*Me$_2$); 1.30 (br s, m O(CH$_2$C*H*$_2$)$_2$); 0.83 (dd, $|^3J_{PH}|$ = 14.3 Hz, $|^3J_{HH}|$ = 7.7 Hz, 9H, PCH(C*H*$_3$)$_2$); 0.79 (dd, $|^3J_{PH}|$ = 14.7 Hz, $|^3J_{HH}|$ = 7.7 Hz, 9H, PCH(C*H*$_3$)$_2$); 0.22 (s, 3H, AlMe); 0.09 (s, 3H, AlMe); −0.02 (s, 6H, AlMe); −0.17 (s, 6H, AlMe); −0.34 (s, 3H, AlMe); −0.38 (s, 9H, AlMe). ^{31}P{^{1}H} NMR (C_6D_6, δ ppm): 48.3. ^{13}C{^{1}H} NMR (C_6D_6, δ ppm): 312.4 (s, Ti(*C*)Al$_3$); 109.7 (s, *Cp*); 68.5 (br s, O(*C*H$_2$CH$_2$)$_2$); 27.2 (d, $|^1J_{PC}|$ = 58.8 Hz, P*C*HMe$_2$); 25.4 (s, O(CH$_2$*C*H$_2$)$_2$); 17.2 (d, $|^2J_{PC}|$ = 44.1 Hz, PCH$_2$(*C*H$_3$)$_2$); 10.4 (s, Ti-*C*H$_3$); −1.1, −2.9, −5.0, −8.8 (AlMe). **[13]14** Yield: >95% by ^{1}H NMR. ^{1}H NMR (C_6D_6, δ ppm): 6.25 (s, 5H, Cp-*H*); 1.92 (sept., $|^3J_{HH}|$ = 7.1 Hz, 3H, PC*H*Me$_2$); 0.88 (dd, $|^3J_{PH}|$ = 14.2 Hz, $|^3J_{HH}|$ = 7.1 Hz, 9H, PCH(C*H*$_3$)$_2$); 0.84 (dd, $|^3J_{PH}|$ = 14.3 Hz, $|^3J_{HH}|$ = 7.1 Hz, 9H, PCH(C*H*$_3$)$_2$); 0.12 (s, 3H, AlMe); −0.17 (s, 6H, AlMe); −0.22 (s, 6H, AlMe); −0.44 (s, 3H, AlMe); −0.47 (s, 9H, AlMe). ^{31}P{^{1}H} NMR (C_6D_6, δ ppm): 48.3 (s, N=*P*(*i*Pr)$_3$); −54.7 (br s, *P*Me$_3$). ^{13}C{^{1}H} NMR (C_6D_6, δ ppm): 309.1 (s, Ti(*C*)Al$_3$); 109.6 (s, *Cp*); 27.2 (d, $|^1J_{PC}|$ = 58.8 Hz, P*C*HMe$_2$); 17.2 (d, $|^2J_{PC}|$ = 40.4 Hz, PCH$_2$(*C*H$_3$)$_2$); 12.8 (br s, P(*C*H$_3$)$_3$); 10.5 (s, Ti-*C*H$_3$); 1.4, 0.3, −0.7, −2.7, −4.1, −4.6, −9.7 (AlMe).

EHMO and MMX Calculations. Extended Huckel molecular orbital (EHMO) and molecular mechanics (MMX) calculations were performed on a Pentium workstation employing the CACHE software package. Models were constructed on the basis of idealized geometries derived from related crystallographic data.

X-ray Data Collection and Reduction. X-ray quality crystals of **7**, **8**, **10**, **11**, **13**, and **15** were obtained directly from the preparation as described above. The crystals were manipulated and mounted in capillaries in a glovebox, thus maintaining a dry, O_2-free environment for each crystal. Diffraction experiments were performed on a Siemens SMART System CCD diffractometer collecting a hemisphere of data in 1329 frames with 10 s exposure times. Crystal data are summarized in Table 1. The observed extinctions were consistent with the space groups in each case. The data sets were collected (4.5° < 2θ < 45−50.0°). A measure of decay was obtained by re-collecting the first 50 frames of each data set. The intensities of reflections within these frames showed no statistically significant change over the duration of the data collections. The data were processed using the SAINT and XPREP processing packages. An empirical absorption correction based on redundant data was applied to each data set. Subsequent solution and refinement was performed using the SHELXTL solution package operating on a SGI Indy Computer. The reflections with $F_o^2 > 3\sigma F_o^2$ were used in the refinements.

Structure Solution and Refinement. Non-hydrogen atomic scattering factors were taken from the literature tabulations.[24] The heavy atom positions were determined using direct methods employing either the SHELXTL or direct methods routines. The remaining non-hydrogen atoms were located from successive difference Fourier map calculations. The refinements were carried out by using full-matrix least-squares techniques on *F*, minimizing the function $w(|F_o| - |F_c|)^2$, where the weight *w* is defined as $4F_o^2/2\sigma(F_o^2)$ and F_o and F_c are the observed and calculated structure factor amplitudes. In the final cycles of each refinement, all non-hydrogen atoms were assigned anisotropic temperature factors. Carbon-bound hydrogen atom positions were calculated and allowed to ride on the carbon to which they are bonded assuming a C−H bond length of 0.95 Å. Hydrogen atom temperature factors were fixed at 1.10 times the isotropic temperature factor of the carbon atom to which they are bonded. The hydrogen atom contributions were calculated, but not refined. The final values of refinement parameters are given in Table 1. The locations

(24) Cromer, D. T.; Mann, J. B. *Acta Crystallogr. A* **1968**, *A24*, 390.

Scheme 1

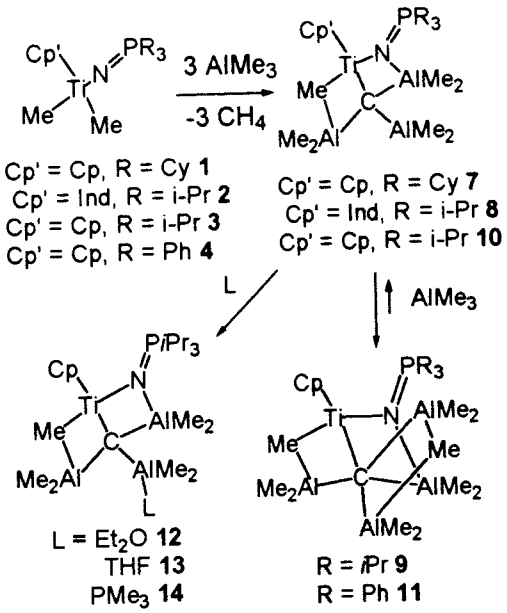

of the largest peaks in the final difference Fourier map calculation as well as the magnitude of the residual electron densities in each case were of no chemical significance. Positional parameters, hydrogen atom parameters, thermal parameters, and bond distances and angles have been deposited as Supporting Information.

Results and Discussion

Reactions of $Cp(Cy_3PN)TiMe_2$, **1**, or (indenyl)(i-Pr_3PN)-$TiMe_2$, **2**, with greater than 3 equiv of $AlMe_3$ in toluene proceeds over a 12 h period to produce the red crystalline products of **7** and **8**, respectively (Scheme 1). In both cases, the yield of isolated product is 72%. ^1H, $^{31}P\{^1H\}$, and $^{13}C\{^1H\}$ NMR data were consistent with the presence of cyclopentadienyl or indenyl and phosphinimide ligands, as well as five apparent methyl environments. While these data did not provide a definitive formulation of the products, crystallographic studies of **7** and **8** confirmed the formulation of these products as CpTi-(μ^2-Me)(μ^2-$NPCy_3$)(μ^4-C)($AlMe_2$)$_3$, **7** (Figure 1), and (indenyl)CpTi(μ^2-Me)(μ^2-NPi-Pr_3)(μ^4-C)($AlMe_2$)$_3$, **8** (Figure 2), respectively. In each case, the pseudo "three-legged piano stool" coordination sphere of Ti is comprised of a cyclopentadienyl or indenyl ring, a methyl group, a phosphinimide nitrogen atom, and a carbide carbon atom. Three aluminum atoms complete the bonding sphere of the carbides. Two $AlMe_2$ moieties bridge the titanium-bound methyl groups and the titanium-bound phosphinimide nitrogen atoms to the carbide carbon atoms, while the respective third $AlMe_2$ fragments occupy terminal positions on the carbides and adopt planar, pseudo-trigonal geometries at the Al centers. The most interesting feature is the geometry about the carbide carbon atoms. The Ti−carbide distances of 1.891(6) and 1.878(4) Å in **7** and **8**, respectively, are significantly shorter than the terminal Ti−CH_3 distance in Cp(t-Bu_3PN)TiMe(μ^2-$CH_3B(C_6F_5)_3$) (2.123(5) Å).[22] These relatively short Ti−C distances are in contrast to the Ti−C(7) and Ti−C(20) distances of 2.257(11) and 2.241(4) Å in **7** and **8**, respectively. These latter carbons bridge the Ti and Al(1) centers with Al−C distances of 2.206(10) and 2.204(5) Å, respectively. In a similar manner the bridging nature of the phosphinimide nitrogen atoms results in Ti−N bond lengths (**7**, 1.998(5); **8**, 1.981(3) Å) that are longer that those seen for complexes of the form $CpTi(NPR_3)Cl_2$.[22,25] The bridging Al−N bond lengths (**7**, 1.920(5); **8**, 1.921(3) Å) are similar to those seen in Al−phosphinimide dimers.[26]

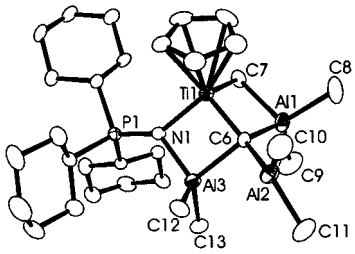

Figure 1. ORTEP drawings of **7**, 20% thermal ellipsoids are shown. Hydrogen atoms have been omitted for clarity. Bond distances (Å) and angles (deg): Ti(1)−C(6) 1.891(6); Ti(1)−N(1) 1.998(5); Ti(1)−C(7) 2.257(11); Al(1)−C(8) 1.968(9); Al(1)−C(9) 1.975(9); Al(1)−C(6) 1.986(7); Al(1)−C(7) 2.206(10); Al(2)−C(6) 1.925(7); Al(2)−C(11) 1.952(8); Al(2)−C(10) 1.953(9); Al(2)−Al(3) 2.941(3); Al(3)−N(1) 1.920(5); Al(3)−C(13) 1.980(7); Al(3)−C(6) 2.043(7); Al(3)−C(12) 2.067(7); P(1)−N(1) 1.597(5); C(6)−Ti(1)−N(1) 93.5(2); C(6)−Ti(1)−C(7) 97.0(3); N(1)−Ti(1)−C(7) 107.5(4); C(8)−Al(1)−C(6) 116.0(4); C(9)−Al(1)−C(6) 116.7(4); C(6)−Al(1)−C(7) 95.9(4); C(6)−Al(2)−C(11) 120.1(4); C(6)−Al(2)−C(10) 122.7(3); N(1)−Al(3)−C(6) 91.3(2); C(13)−Al(3)−C(6) 120.2(3); C(6)−Al(3)−C(12) 100.5(3); P(1)−N(1)−Al(3) 130.0(3); P(1)−N(1)−Ti(1) 141.9(3); Al(3)−N(1)−Ti(1) 87.7(2); Ti(1)−C(6)−Al(2) 143.1(4); Ti(1)−C(6)−Al(1) 89.8(3); Al(2)−C(6)−Al(1) 118.6(3); Ti(1)−C(6)−Al(3) 87.2(2); Al(2)−C(6)−Al(3) 95.6(3); Al(1)−C(6)−Al(3) 121.8(3); Al(1)−C(7)−Ti(1) 75.7(3)

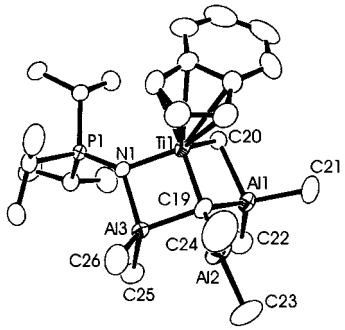

Figure 2. ORTEP drawings of **8**, 20% thermal ellipsoids are shown. Hydrogen atoms have been omitted for clarity. Bond distances (Å) and angles (deg): Ti(1)−C(19) 1.878(4); Ti(1)−N(1) 1.981(3); Ti(1)−C(20) 2.241(4); Al(1)−C(21) 1.969(5); Al(1)−C(22) 1.970(5); Al(1)−C(19) 1.989(4); Al(1)−C(20) 2.204(5); Al(2)−C(19) 1.922(4); Al(2)−C(23) 1.948(8); Al(2)−C(24) 1.964(9); Al(3)−N(1) 1.921(3); Al(3)−C(25) 1.953(8); Al(3)−C(19) 2.030(5); Al(3)−C(26) 2.039(8); P(1)−N(1) 1.601(3); C(19)−Ti(1)−N(1) 93.82(16); C(19)−Ti(1)−C(20) 96.67(17); N(1)−Ti(1)−C(20) 106.16(14); C(21)−Al(1)−C(19) 116.8(2); C(22)−Al(1)−C(19) 118.5(2); C(19)−Al(1)−C(20) 94.70(16); C(19)−Al(2)−C(23) 119.0(4); C(19)−Al(2)−C(24) 123.6(3); N(1)−Al(3)−C(19) 90.99(15); C(25)−Al(3)−C(19) 120.4(3); C(19)−Al(3)−C(26) 102.0(3); N(1)−P(1)−C(16) 110.19(18); N(1)−P(1)−C(13) 112.8(2); C(16)−P(1)−C(13) 105.7(2); P(1)−N(1)−Al(3) 129.60(19); P(1)−N(1)−Ti(1) 142.65(18); Al(3)−N(1)−Ti(1) 87.67(13); Ti(1)−C(19)−Al(2) 139.7(3); Ti(1)−C(19)−Al(1) 90.67(17); Al(2)−C(19)−Al(1) 118.9(2); Ti(1)−C(19)−Al(3) 87.42(16); Al(2)−C(19)−Al(3) 99.5(2); Al(1)−C(19)−Al(3) 118.7(2); Al(1)−C(20)−Ti(1) 76.49(13).

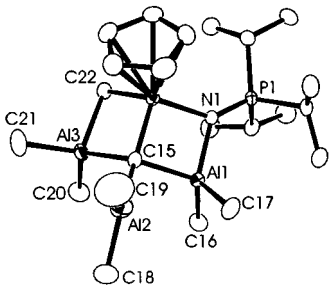

Figure 3. ORTEP drawings of **10**, 20% thermal ellipsoids are shown. Hydrogen atoms have been omitted for clarity. Bond distances (Å) and angles (deg): Ti(1)−C(15) 1.878(4); Ti(1)−N(1) 1.983(3); Ti(1)−C(22) 2.290(5); P(1)−N(1) 1.606(3); Al(1)−N(1) 1.925(3); Al(1)−C(16) 1.960(5); Al(1)−C(17) 2.020(5); Al(1)−C(15) 2.035(4); Al(2)−C(15) 1.912(4); Al(2)−C(18) 1.950(7); Al(2)−C(19) 1.983(8); Al(3)−C(20) 1.969(6); Al(3)−C(21) 1.987(5); Al(3)−C(15) 2.011(4); Al(3)−C(22) 2.165(5); C(15)−Ti(1)−N(1) 93.51(13); C(15)−Ti(1)−C(22) 96.52(17); N(1)−Ti(1)−C(22) 108.49(16); N(1)−Al(1)−C(15) 90.51(14); C(16)−Al(1)−C(15) 119.0(2); C(17)−Al(1)−C(15) 102.5(2); C(15)−Al(2)−C(18) 119.9(3); C(15)−Al(2)−C(19) 121.1(3); C(20)−Al(3)−C(15) 117.4(2); C(21)−Al(3)−C(15) 112.6(2); C(15)−Al(3)−C(22) 96.70(17); P(1)−N(1)−Al(1) 130.40(16); P(1)−N(1)−Ti(1) 141.38(17); Al(1)−N(1)−Ti(1) 88.05(11); Ti(1)−C(15)−Al(2) 145.5(2); Ti(1)−C(15)−Al(3) 89.09(16); Al(2)−C(15)−Al(3) 111.89(18); Ti(1)−C(15)−Al(1) 87.83(14); Al(2)−C(15)−Al(1) 101.76(17); Al(3)−C(15)−Al(1) 122.76(19); Al(3)−C(22)−Ti(1) 75.53(15).

The geometry about the carbide carbon is that of a somewhat flattened tetrahedron, as evidenced by the Ti−C−Al2 and Al1−C−Al3 angles: **7**, 143.1(4)°, 121.8(3)°; **8**, 139.7(3)°, 118.7(2)°.

The analogous reaction of Cp(*i*-Pr_3PN)$TiMe_2$, **3**, with greater than 4 equiv of $AlMe_3$ in toluene or hexane proceeds over a 16 h period to produce a red product **9** isolated in 67% yield. Compound **9** gives rise to a single resonance in the $^{31}P\{^1H\}$ NMR spectrum at 50.9 ppm, and ^1H and ^{13}C NMR spectra were consistent with the presence of cyclopentadienyl and phosphinimide ligands. In contrast to **7** and **8**, compound **9** exhibits four broad resonances near 0 ppm in the ^1H NMR spectrum for the $AlMe_x$ protons integrating to 30 hydrogen atoms, suggesting a 4:1 combination of Al and Ti in **9**. Recrystallization of **9** from benzene afforded crystals of a slightly different species, **10**, with a single resonance in the $^{31}P\{^1H\}$ NMR spectrum at 49.8 ppm and slightly altered ^1H and ^{13}C NMR spectra. This species exhibits three broad resonances near 0 ppm in the ^1H NMR spectrum, which integrate to 21 protons. $^{27}Al\{^1H\}$ NMR spectral data also reveal three broad resonances at 149, 114, and 38 ppm, suggesting a 3:1 combination of Al and Ti in the product. The identity of **10** was confirmed crystallographically as [CpTi(μ^2-Me)(μ^2-NP*i*-Pr_3)(μ^4-C)($AlMe_2$)$_3$]- (Figure 3). The molecular features and metric parameters of **10** varied only slightly from those described above for **7** and **8**.

Resonances attributable to the carbide carbon atoms of **7**, **8**, **9**, and **10** were not observed in initial $^{13}C\{^1H\}$ NMR spectra. This was attributed to the long relaxation time of the quaternary carbon atom, the quadrapolar nature of Al atoms bonded to the carbide, and the low natural abundance of the ^{13}C isotope. To facilitate observation of the carbide carbon atom in the $^{13}C\{^1H\}$ NMR spectrum, and perhaps gain mechanistic insight into the formation of the clusters, preparation of the labeled species Cp(*i*-Pr_3PN)Ti(^{13}Me)$_2$, **^{13}3**, was undertaken employing ^{13}MeMgBr. Subsequent reaction with $AlMe_3$ gave ^{13}C-labeled **9**. A resonance observed at 298.1 ppm in the $^{13}C\{^1H\}$ NMR spectrum of **^{13}9** at 25° C was attributed to the carbide carbon. It is also noteworthy that in the formation of **^{13}9** methyl exchange between the Ti−Me and Al−Me groups presumably prior to C−H bond activation resulted in a random distribution of ^{13}C atoms in the carbide, Al−Me, and Ti−Me sites. This scrambling provides sufficient enrichment to reveal the carbide ^{13}C resonance of **^{13}10** at 304.7 ppm.

A variable-temperature NMR study of ^{13}**9** with 3 equiv of $AlMe_3$ showed a dramatic upfield shift in the carbide resonance to 241.2 ppm in d_8-toluene at 260 K. This, together with the ^1H NMR data, supports the proposition that an equilibrium between **^{13}10** and $AlMe_3$ (Scheme 2) affords **^{13}9** in solution at low temperature with the formulation of **9** as [CpTi(μ^2-Me)(μ^2-NP*i*-Pr_3)-(μ^5-C)($AlMe_2$)$_3$·($AlMe_3$)]. The equilibrium constant for eq 1 was determined by variable-temperature $^{31}P\{^1H\}$ NMR to be 129 M^{-1} at 260 K. The corresponding thermodynamic parameters are ΔG(260 K) = −10.5 kJ mol^{-1}, ΔH = −57.9 kJ mol^{-1}, and ΔS = −0.183 kJ $mol^{-1}K^{-1}$.

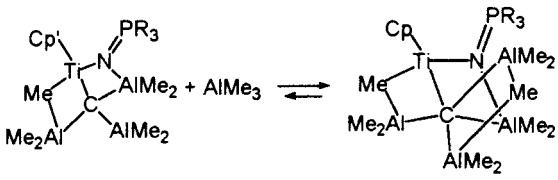

(1)

The nature of the interaction with the additional equivalent of $AlMe_3$ in **9** was illuminated by the reaction of [CpTi(NPPh_3)Me_2], **4**, with excess $AlMe_3$. The product **10**, isolated in 64% yield, gives rise to a single resonance in the $^{31}P\{^1H\}$ NMR spectrum at 25.2 ppm, while its ^1H NMR data suggest a formulation analogous to **9**, i.e., [CpTi(μ^2-Me)(μ^2-NPPh_3)(μ^5-C)($AlMe_2$)$_3$·($AlMe_3$)], **11**. Crystallographic studies of **11** confirmed this formulation (Figure 4). The core structural features of the molecule **11** are similar to those described above for **7**, **8**, and **10**. However an additional equivalent of $AlMe_3$ bridges the central $AlMe_2$ fragment and the carbide via Lewis acid−base interactions. This results in a five-coordinate carbide center. The geometry about this carbide carbon atom is distorted trigonal bipyramidal, with the Ti−C(24)−Al(4) vector essentially linear (175.80(16)°). Three Al atoms comprise the pseudoequatorial plane. These atoms adopt angles ranging from 78.12(11)° to 104.81(13)° with respect to the pseudoaxial atoms. Angles within the trigonal plane vary from 114.36(14)° to 130.72(15)°. These distortions are consistent with the presence of strain arising from two fused four-membered Ti−C−Al−C and Ti−C−Al−N rings in these complexes. The isolation and characterization of compounds **9**−**11** demonstrates a rare example of four- and five-coordinate quaternary and quinternary carbon atoms. In this regard, Schmidbaur et al.[27] have described a C_{3v} symmetric gold carbocation $[(Ph_3PAu)_5C]^+$ which contains five-coordinate carbide. Computational studies for the

(25) Dehnicke, K.; Strahle, J. *Polyhedron* **1989**, *8*, 707−726.
(26) Ong, C. M.; McKarns, P.; Stephan, D. W. *Organometallics* **1999**, *18*, 4197−4204.

Scheme 2

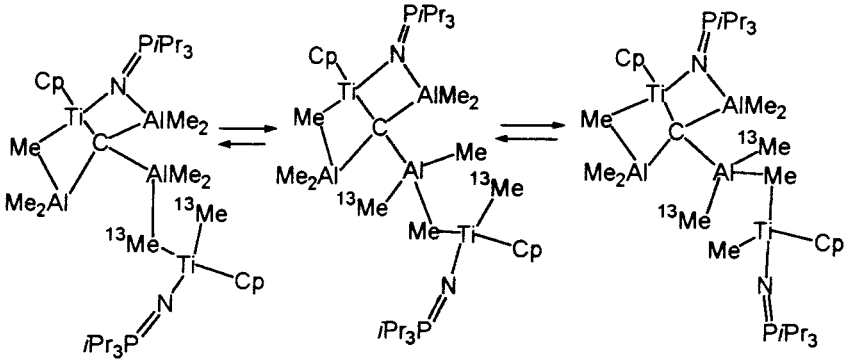

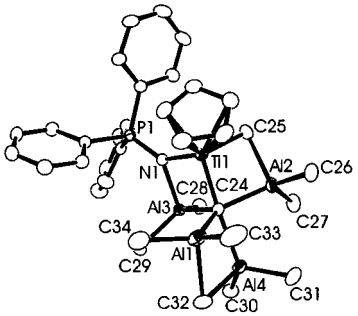

Figure 4. ORTEP drawings of **11**, 20% thermal ellipsoids are shown. Hydrogen atoms have been omitted for clarity. Bond distances (Å) and angles (deg): Ti(1)−N(1) 1.942(2); Ti(1)−C(24) 1.972(3); Ti(1)−C(25) 2.237(4); Al(1)−C(33) 1.976(5); Al(1)−C(34) 1.977(5); Al(1)−C(24) 2.087(3); Al(1)−C(32) 2.228(4); Al(1)−Al(4) 2.6519(15); Al(2)−C(26) 1.964(4); Al(2)−C(27) 1.968(4);Al(2)−C(24) 2.095(3); Al(2)−C(25) 2.202(4); Al(3)−N(1) 1.943(2); Al(3)−C(28) 1.972(3); Al(3)−C(29) 1.984(3); Al(3)−C(24) 2.150(3); Al(4)−C(30) 1.976(4); Al(4)−C(31) 1.987(4); Al(4)−C(24) 2.121(3); Al(4)−C(32) 2.154(4); P(1)−N(1) 1.598(2); N(1)−Ti(1)−C(24) 95.10(11); N(1)−Ti(1)−C(25) 97.83(13); C(24)−Ti(1)−C(25) 95.70(14); C(33)−Al(1)−C(34) 114.2(2); C(33)−Al(1)−C(24) 116.1(2); C(34)−Al(1)−C(24) 121.69(16); C(24)−Al(1)−C(32) 100.24(14); C(26)−Al(2)−C(24) 120.34(17); C(27)−Al(2)−C(24) 117.03(15); C(24)−Al(2)−C(25) 93.30(13); N(1)−Al(3)−C(24) 89.60(11); C(28)−Al(3)−C(24) 118.30(14); C(29)−Al(3)−C(24) 112.61(14); N(1)−Al(3)−Ti(1) 44.84(7); C(30)−Al(4)−C(24) 118.90(15); C(31)−Al(4)−C(24) 114.54(16); C(24)−Al(4)−C(32) 101.57(14); P(1)−N(1)−Ti(1) 139.22(14); P(1)−N(1)−Al(3) 130.46(14); Ti(1)−N(1)−Al(3) 90.30(10); Ti(1)−C(24)−Al(1) 104.81(13); Ti(1)−C(24)−Al(2) 84.08(11); Ti(1)−C(24)−Al(3) 83.72(11); Ti(1)−C(24)−Al(4) 175.80(16); Al(1)−C(24)−Al(2) 130.72(15); Al(1)−C(24)−Al(3) 114.36(14); Al(1)−C(24)−Al(4) 78.12(11); Al(2)−C(24)−Al(4) 91.73(11); Al(2)−C(24)−Al(3) 114.77(14); Al(4)−C(24)−Al(3) 97.87(12); Al(2)−C(25)−Ti(1) 75.73(13).

cations $[CH_5]^+$ and $[CLi_5]^+$ have predicted similar geometries.[28] In very recent work, Akiba and co-workers have described the hypervalent organic carbocation $[(MeO)_2C((MeO)_2C_{14}H_7)]^+$.[29]

The reaction of **10** with $AlMe_3$ to form the adduct **9** indicates that the four-coordinate carbide complexes retain Lewis acidity at the planar three-coordinate Al center (Al2). This view is confirmed in the reactions of **9** with diethyl ether, THF, or PMe_3, which yield the species $[CpTi(\mu^2\text{-Me})(\mu^2\text{-NP}i\text{-Pr}_3)(\mu^4\text{-C})(AlMe_2)_2(AlMe_2(L))]$ (L = Et_2O **12**, THF **13**, PMe_3 **14**) (Scheme 1). The Al−Me resonances in the ^1H NMR spectra of these species are much sharper than those of **7**−**11**, presumably as coordination of the donor to Al2 precludes the methyl exchange processes between adjacent $AlMe_2$ sites. Employing the precursor ^{13}**9**, the $^{13}C\{^1H\}$ NMR resonance for the carbide atom in the donor adducts **12**−**14** was observed shifted downfield to 309.1−312.8 ppm.

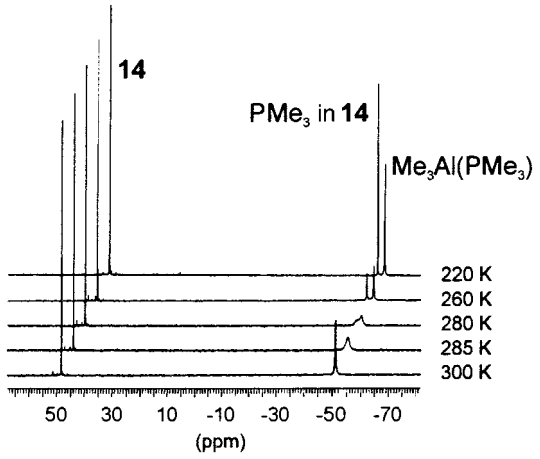

Figure 5. Variable-temperature $^{31}P\{^1H\}$ NMR spectra of **14**.

Stoichiometric reactions of **9** with PMe_3 were monitored by variable-temperature $^{31}P\{^1H\}$ NMR spectroscopy in d_8-toluene (Figure 5). Upon reaction of 2 equiv with **9**, a single broad resonance is observed for PMe_3 at −51.1 ppm at 300 K. After cooling to 220 K, this resonance is split into two signals in the ratio 1:1. The signal at −49.2 ppm corresponds to the PMe_3 in **14**. The remaining signal at −51.7 ppm arises from $AlMe_3$-bound PMe_3. Compound **14** was isolated and crystallographically characterized (Figure 6). The gross structural features of **14** were similar to those seen for **10** with the addition of coordination of phosphine to Al(2), which adopts a pseudo-tetrahedral geometry. Small differences in the metric parameters were observed in the Ti−C distance and geometry about the carbide carbon.

Extended Hückel molecular orbital calculations were performed on the model compound $CpTi(\mu^2\text{-Me})(\mu^2\text{-NPH}_3)(\mu^5\text{-C})(AlMe_2)_3$ constructed from crystallographic data. The three highest occupied molecular orbitals are principally carbide carbon based p-orbitals. This local-

(27) Scherbaum, F.; Grohmann, A.; Muller, G.; Schmidbaur, H. *Angew. Chem., Int. Ed. Engl.* **1989**, *28*, 463.
(28) Jemmis, E. D.; Chandrasekhar, J.; Würthwein, E.-U.; Schleyer, P. v. R.; Chinn, J. W. J.; Landro, F. J.; Lagow, R. J.; Luke, B.; Pople, J. A. *J. Am. Chem. Soc.* **1982**, *104*, 4275.
(29) Akiba, K.-Y.; Yamashita, M.; Yamamoto, Y.; Nagase, S. *J. Am. Chem. Soc.* **1999**, *121*, 10644−10645.

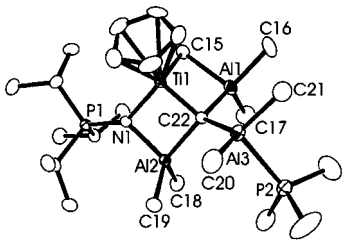

Figure 6. ORTEP drawings of **14**, 20% thermal ellipsoids are shown. Hydrogen atoms have been omitted for clarity. Bond distances (Å) and angles (deg): Ti(1)−C(22) 1.887(5); Ti(1)−N(1) 1.971(4); Ti(1)−C(15) 2.288(9); Al(1)−C(16) 1.969(7); Al(1)−C(17) 1.982(7); Al(1)−C(22) 2.016(6); Al(1)−C(15) 2.215(9); Al(2)−N(1) 1.940(5); Al(2)−C(18) 1.976(6); Al(2)−C(19) 1.982(7); Al(2)−C(22) 2.060(5); Al(3)−C(20) 1.977(7); Al(3)−C(22) 1.987(6); Al(3)−C(21) 1.995(7); Al(3)−P(2) 2.517(3); P(1)−N(1) 1.613(4); C(22)−Ti(1)−N(1) 95.0(2); C(22)−Ti(1)−C(15) 98.0(3); N(1)−Ti(1)−C(15) 102.9(3); C(22)−Al(1)−C(15) 96.6(3); N(1)−Al(2)−C(22) 90.6(2); C(22)−Al(3)−P(2) 107.54(17); C(21)−Al(3)−P(2) 96.7(2); P(1)−N(1)−Al(2) 130.5(2); P(1)−N(1)−Ti(1) 141.7(3); Al(2)−N(1)−Ti(1) 87.71(17); Al(1)−C(15)−Ti(1) 74.9(3); Ti(1)−C(22)−Al(3) 132.4(3); Ti(1)−C(22)−Al(1) 89.0(2); Al(3)−C(22)−Al(1) 112.0(2); Ti(1)−C(22)−Al(2) 86.6(2); Al(3)−C(22)−Al(2) 117.8(3); Al(1)−C(22)−Al(2) 115.1(3).

Scheme 3

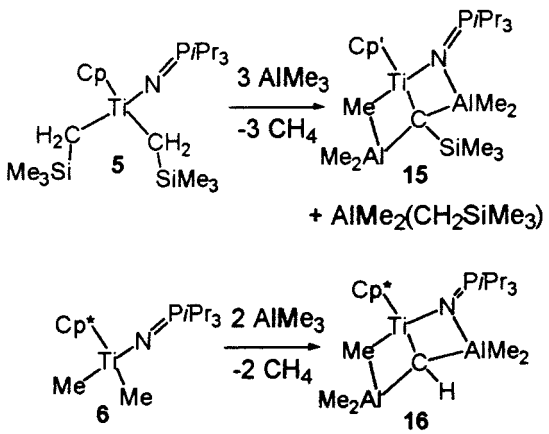

ized electron density presumably accounts for the interaction of the carbide with the Lewis acidic Al center in the formation of the five-coordinate carbide complexes **9** and **11**. On the other hand, the three LUMOs for the model compound are comprised principally of Ti-based d-orbitals, while the LUMO+3 is localized on the central planar Al atom. On this basis, nucleophilic attack at Ti would be anticipated. However, the formation of **12**−**14** clearly demonstrates donor coordination at the central Al atom. This infers that steric congestion precludes complexation at Ti in favor of the more accessible Al center.

Attempts to exploit the Lewis acidity of **10** at 25 °C were undertaken, and as **9** and **10** are in equilibrium, use of ^{13}**9** provides a ready source of ^{13}**10**. Keeping in mind that the carbide, Ti−Me, and Al−Me groups of ^{13}**9** are statistical distributions of *both* ^{12}C and ^{13}C isotopes, ^{13}**9** was reacted with fully labeled ^{13}**3** in a NMR tube experiment. Spectroscopic data revealed the formation of a 1:1 adduct of **10** and **3**. In particular the ^{1}H NMR spectrum showed titanium-bound methyl resonances in ^{13}**3** attributable to *both* ^{12}C (singlet) and ^{13}C methyl groups (d, $|^{1}J_{CH}| = 119$ Hz). This observation

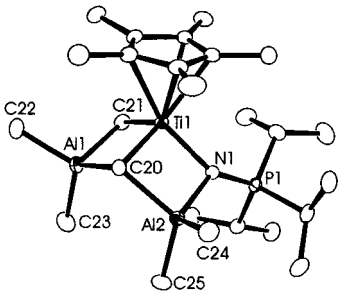

Figure 7. ORTEP drawings of **16**, thermal ellipsoids are shown. Hydrogen atoms have been omitted for clarity. Bond distances (Å) and angles (deg): Ti(1)−C(20) 1.900(2); Ti(1)−N(1) 2.0036(17); Ti(1)−C(21) 2.293(2); Al(1)−C(23) 1.977(3); Al(1)−C(22) 1.979(3); Al(1)−C(20) 2.043(2); Al(1)−C(21) 2.157(3); Al(2)−N(1) 1.9482(17); Al(2)−C(25) 1.978(3); Al(2)−C(24) 1.988(3); Al(2)−C(20) 2.059(2); P(1)−N(1) 1.5981(17); C(20)−Ti(1)−N(1) 92.99(8); C(20)−Ti(1)−C(21) 97.78(9); N(1)−Ti(1)−C(21) 104.20(8); C(20)−Al(1)−C(21) 97.94(9); N(1)−Al(2)−C(20) 89.89(8); P(1)−N(1)−Al(2) 126.93(10); P(1)−N(1)−Ti(1) 143.92(10); Al(2)−N(1)−Ti(1) 88.12(7); Ti(1)−C(20)−Al(1) 87.92(9); Ti(1)−C(20)−Al(2) 87.84(8); Al(1)−C(20)−Al(2) 117.85(11).

affirms a facile process whereby Ti−^{13}CH$_3$ of ^{13}**3** and carbide−Al−^{12}CH$_3$ groups of ^{13}**10** exchange. Although this adduct was not isolable, a proposed structure is shown in Scheme 2. Apart from this exchange mechanism, no evidence for additional processes such as methyl group abstraction from ^{13}**3** by the AlMe$_2$ group was observed.

The effect of sterics on the course of the C−H activation reaction was also investigated. Reaction of Cp(*i*-Pr$_3$PN)Ti(CH$_2$SiMe$_3$)$_2$, **5**, with AlMe$_3$ afforded the product **15** (Scheme 3). The NMR data supported the inclusion of a single SiMe$_3$ and five methyl groups in **15**, resulting in the formulation of the product as CpTi(μ^2-Me)(μ^2-NP*i*-Pr$_3$)(μ^3-CSiMe$_3$)(AlMe$_2$)$_2$, **15**. In a similar fashion, reaction of Cp*(*i*-Pr$_3$PN)TiMe$_2$, **6**, with AlMe$_3$ proceeded to give the product **16**. In addition to the other spectroscopic data, the direct observation of the non-^{13}C-enriched methine resonance at 241 ppm in the ^{13}C NMR spectrum suggested the formulation of **16** as Cp*Ti(μ^2-Me)(μ^2-NP*i*-Pr$_3$)(μ^3-CH)(AlMe$_2$)$_2$. A crystallographic study (Figure 7) revealed that only 2 equiv of AlMe$_3$ reacted with **6**, resulting in double C−H bond activation and leaving the methine proton unreacted. It is presumed that the steric congestion offered by the pentamethylcyclopentadienyl ligand inhibits the activation of the methine proton.

Conclusions

The isolation and characterization of the above carbide complexes has two important implications. First, we have previously described the active olefin polymerization catalysts derived from compounds **1**−**4** upon activation with borate salts. In contrast, activation with methylalumoxane results in much less active species. Monitoring reactions of CpTi(NP*i*-Pr$_3$)Cl$_2$ with MAO by ^{31}P{^{1}H} NMR after 72 h at 25 °C reveals a group of resonances in the same range as those seen for the carbide species described above. This suggests the possibility that C−H bond activation may be a degradation pathway for these catalysts. While this may account for the degradation products during MAO-activated

polymerizations, it may also be that simple dative interaction of the Ti-bound phosphinimide ligand with an Al species is sufficient to suppress catalyst activity.

The second implication of this work relates to C−H bond activation. The products described herein suggest a role for Ti-bound ancillary phosphinimide ligands in initiating the Ti−Al interaction. Although this phenomenon appears to be general for these Ti−phosphinimide complexes, it does prompt an even more general question: can ancillary ligands initiate interactions with Lewis acids and thus precipitate C−H bond activation chemistry? In this regard, we are continuing to study the chemistry of phosphinimide complexes. In addition, the potential for synthetic utility of the products of C−H bond activation is the subject of ongoing investigations.

Acknowledgment. Financial support from the NOVA Chemicals Corporation and NSERC of Canada is gratefully acknowledged. F.G. is grateful for the award of an NSERC postdoctoral fellowship.

Supporting Information Available: Spectroscopic and crystallographic data. This material is available free of charge via the Internet at http://pubs.acs.org.

OM001047W